Drug Deliv. and Transl. Res. (2016) 6:148–158
DOI 10.1007/s13346-015-0224-4

RESEARCH ARTICLE

Riboflavin-induced photo-crosslinking of collagen hydrogel and its application in meniscus tissue engineering

Jiseung Heo[1] · Rachel H. Koh[1] · Whuisu Shim[2] · Hwan D. Kim[1] · Hyun-Gu Yim[1] · Nathaniel S. Hwang[1,3]

Published online: 26 March 2015

Abstract A meniscus tear is a common knee injury, but its regeneration remains a clinical challenge. Recently, collagen-based scaffolds have been applied in meniscus tissue engineering. Despite its prevalence, application of natural collagen scaffold in clinical setting is limited due to its extremely low stiffness and rapid degradation. The purpose of the present study was to increase the mechanical properties and delay degradation rate of a collagen-based scaffold by photo-crosslinking using riboflavin (RF) and UV exposure. RF is a biocompatible vitamin B2 that showed minimal cytotoxicity compared to conventionally utilized photo-initiator. Furthermore, collagen photo-crosslinking with RF improved mechanical properties and delayed enzyme-triggered degradation of collagen scaffolds. RF-induced photo-crosslinked collagen scaffolds encapsulated with fibrochondrocytes resulted in reduced scaffold contraction and enhanced gene expression levels for the collagen II and aggrecan. Additionally, hyaluronic acid (HA) incorporation into photo-crosslinked collagen scaffold showed an increase in its retention. Based on these results, we demonstrate that photo-crosslinked collagen-HA hydrogels can be potentially applied in the scaffold-based meniscus tissue engineering.

Keywords Collagen · Hydrogel · Riboflavin · Hyaluronic acid · Meniscus tissue engineering · Fibrochondrocyte

Introduction

Meniscus, a fibrocartilaginous tissue located between knee joints, significantly contributes to knee health by playing a critical role in shock absorption, load distribution, and joint stabilization [1]. Meniscal tissues consist of water (72 %), collagen fiber (22 %), and proteoglycan (0.8 %). Their biochemical composition varies depending on the anatomical region of the meniscus with different properties [2, 3]. The outer meniscus is mainly of type I collagen and provides tensile force resistance. The inner meniscus consists of type II collagen and proteoglycan, and this region plays a critical role in shock absorption [4, 5].

Meniscus tear is known to occur readily with aging or extreme exercising. When meniscus tear occurs, the inner meniscus region has limited regeneration capacity since it is an avascular tissue with limited self-healing ability [6]. In the past, meniscus was considered an unimportant tissue residue generated during joint formation. However, recent studies have revealed that removal of the meniscus amplifies degenerative arthritis development and thus have emphasized its importance in joint tissue homeostasis [7]. Numerous studies have been conducted to develop a treatment for meniscus tears. Some of the major approaches are allograft transplantation, meniscectomy, and meniscus substitution [8, 9].

Electronic supplementary material The online version of this article (doi:10.1007/s13346-015-0224-4) contains supplementary material, which is available to authorized users.

✉ Nathaniel S. Hwang
nshwang@snu.ac.kr

[1] School of Chemical and Biological Engineering, Institute of Chemical Processes, Seoul National University, 1 Gwanak-ro, Gwanak-gu, Seoul 151-742, South Korea

[2] Department of Materials Science and Engineering, Virginia Polytechnic Institute and State University, Blacksburg, VA, USA

[3] N-BIO Institute, Seoul National University, Seoul, South Korea

Although such treatments have shown little improvements on regenerating the meniscus, the progress seems to be very limited with lack of qualified tissues for long-term stable treatment.

One of the promising alternatives is scaffold-based tissue engineering. Scaffold-based tissue engineering provides material-driven tissue regeneration through bioactive scaffold fabrication. For ideal meniscus tissue engineering, it is required to develop a scaffold that fits properly to the meniscus. Scaffold that guides cells to regenerate functional tissue should be both biocompatible and able to induce synthesis of meniscal ECM component such as type I collagen, type II collagen, and proteoglycan. Also, excessive degradation of the scaffold should not be reached until complete tissue regeneration.

In tissue engineering, collagen is being widely utilized as biomaterial due to its abundance, biocompatibility, and ease of incorporation into new tissue matrix. Collagen is soluble in acids and becomes hydrogel forming self-assembly triple helix structure at 37 °C with the neutral condition. Since collagen hydrogel is easily manufactured by controlling pH and temperature conditions, collagen-based hydrogel has been commonly used in cell culture. In particular, type I collagen has been studied for biomaterial of the meniscus scaffold since it accounts for 90 % of collagen fiber that existed in the meniscus [10, 11].

However, due to weak mechanical property and rapid degradation, without modification, it is hard to handle collagen hydrogel clinically. Also, cell–collagen interaction leads to contraction of cell-laden collagen-based scaffold, leading to reduced size and shape. Such shrinking property limits its use when used as a defect filler. To overcome this disadvantage, various collagen crosslinking methods, such as glutaraldehyde, formaldehyde, and ECD/NHS, have been utilized [12, 13]. However, well-established methodologies are not yet developed for cell encapsulating collagen scaffold without cytotoxicity.

In this study, we have investigated riboflavin (RF) as a photo-sensitizer for photo-crosslinking of collagen hydrogel scaffold. Combined RF and UV has been proven clinically for strengthening of the collagen layer in the cornea repair [14, 15]. The crosslinking results from the covalent bond formation between amino acid of collagen fibril induced by singlet oxygen generated from light-excited RF [16]. Due to its ability to strengthen collagen with non-cytotoxicity and in situ gelling, researches have gradually utilized this method for development of cell encapsulations. Recent studies by Ahluwalia developed RF-induced collagen hydrogel and examined viability when fibroblasts and chondrocytes were encapsulated [17]. Furthermore, Lee and colleagues have showed substantially improved neocartilage formation through RF-induced crosslinked type II collagen and methacrylated glycol chitosan with TGF-β [18].

The aim of this study was to determine the optimal treatment condition of RF for injectable cell-based collagen scaffold and biosynthetic activity of meniscus cells populated scaffold. In addition, crosslinked hyaluronic acid (HA), which is known to promote meniscus regeneration, was incorporated into the collagen hydrogel [19]. We hypothesized that the cell encapsulated photo-crosslinked collagen gel would have potential for utilization in meniscus regeneration and addition of crosslinked HA would accelerate synthesis of ECM component.

Materials and methods

Chemicals and reagents

All chemicals and reagents were purchased from the following vendors and stored according to the manufacturer's recommendation: bovine type I collagen 3 mg/ml (Advanced Biomatrix), sodium hyaluronate 64 kDa (HA, Lifecore Co.), hexamethylenediamine (HMDA, Sigma), 1-ethyl-3-[3-(dimethyl amino)propyl]carbodiimide (EDC, Thermo Scientific), 1-hydroxybenzotriazole monohydrate(HOBt, GL Biochem Ltd.), sodium hydroxide (NaOH, Sigma), 10× phosphate-buffered saline (PBS, Gibco), 1× phosphate-buffered saline (PBS, Gibco), riboflavin 5′-phosphate sodium salt hydrate (Sigma), fetal bovine serum (FBS, Gibco), Dulbecco's modified Eagle's medium, nutrient mixture F-12 (DMEM/F-12, Gibco), penicillin-streptomycin (Pen strep, Gibco), non-essential amino acid (NEAA, Gibco), vitamin C (Sigma), deuterium oxide (Sigma), type II collagenase (Worthington), hyaluronidase from bovine testes (Sigma), live/dead cell viability/cytotoxicity kit (Molecular Probes, L-3224), optimal temperature cutting compound (OCT, Cell Path Ltd.), Mayer's hematoxylin (Dako), Safranin-O (Polysciencesm, Inc), Eosin Y (Sigma), Masson's trichrome (Sigma), and M-MLV cDNA synthesis kit (Enzynomics).

Fibrochondrocyte isolation and culture

Fibrochondrocytes were isolated from New Zealand white rabbit as described previously [10]. In brief, meniscus tissues were removed from rabbit knee joints, and sterile razor blade was used to dissect the inner rim of the meniscus. Minced meniscus pieces were treated with 0.2 % collagenase in DMEM/F12 supplemented with 10 % FBS, 100 U/ml Pen strep for 16 h. The resulting cells were filtered through 70-μm cell strainers. Isolated cells were then maintained with DMEM/F12, 10 % FBS, 100 U/ml Pen strep, 50 μg/ml vitamin C, and 100 μM NEAA and incubated at 37 °C in 5 % CO_2.

Photo-crosslinking of collagen and cell encapsulation

Collagen hydrogel (0.27 % *w/v*) was prepared by mixing 1 part of 10× PBS with 9 parts of collagen solution (0.3 % *w/v* in 0.01 N acetic acid). Riboflavin solution (for five different final concentrations of 0.001, 0.006, 0.01, 0.02, and 0.1 %) was added and subsequently neutralized with 1 M NaOH. Hydrogels were incubated at 37 °C for 10 min or 20 min followed by UV light (3.5 mW/cm^2) exposure for 1, 3, or 5 min. Collagen hydrogel without riboflavin was used as a control. For fibrochondrocyte encapsulation, cells were gently pipetted with neutralized collagen precursor solution (150 μl) at a concentration of 1×10^6 cells/construct. Next, cell-laden collagen solution with riboflavin was incubated for 20 min and photo-crosslinked for 3 min. In the case of the control group, cell-laden collagen solution was incubated for 1 h. The constructs were cultured for 3 weeks at 37 °C with CO_2 incubation in fibrochondrocyte culture medium.

Synthesis of crosslinked hyaluronic acid

Crosslinked HA was prepared as described [20]. Briefly, 4 % *w/v* of HA in distilled water was mixed with HMDA. The molar ratio of HMDA to the carboxylic group of HA was 1:1. EDC and HOBt were added to the mixed solution of HA and HMDA, followed by incubation at 37 °C for 2 h. After completing crosslinking reaction, hydrogels were dialyzed against 1× PBS for 3 days to eliminate unreacted material and freeze-dried for 2 days. Dried hydrogels were broken down into power and stored at −20 °C. In order to confirm crosslinking of HA, hydrogels were degraded by hyaluronidase (100 U/ml) and ^{1}H NMR analysis was performed. Crosslinked HA was incorporated into the collagen scaffolds for further analysis.

Circular dichroism (CD) measurement

CD spectra were measured for analyzing incubation time-dependent triple helix structure of photo-crosslinked collagen scaffolds. CD detector (AppliedPhotophysics Chirascan Plus) equipped with a 150-W xenon lamp was used for the measurement, and spectrum range was 210 to 250 nm.

Rheological analysis

A strain-controlled rotational rheometer determined viscoelastic properties of hydrogels (TA Instrument, ARES). Hydrogels were prepared in 8 mm diameter and 3 mm height. For frequency sweep measurements, the strain was kept at 0.2 % and the frequency was varied from 0.1 to 100 rad/s. The temperature was maintained at 30.0 °C during the measurement.

Swelling ratio

Hydrogels were swollen in PBS for overnight, and wet weight was measured after removing the surface water with weighing paper. Then, dry weight of freeze-dried hydrogels was measured. Swelling ratio was calculated by the following equation:

$$\text{Swelling ratio}(Q) = \frac{\text{wet } \textit{weight of the equilibrated hydrogel in PBS}}{\text{weight } \textit{of the dried hydrogel}}$$

Live/dead assay and contraction assay

Live/dead cell viability/cytotoxicity kit was used following the manufacturer's protocol. Live cells were stained by green fluorescent calcein AM, and red fluorescent ethidium homodimer-1 (Ethd-1) stained dead cells. Cellular images were collected by a Zeiss LSM 720 confocal microscope. To determine the degree of contraction, cell-laden hydrogel (7×10^5 cells/construct) sizes were measured at various times with ImageJ software.

Scaffold degradation

Hydrogels were treated with 10 U/ml of type I collagenase. Time course data were collected by measuring weight of remaining hydrogels (n=3), changing fresh collagenase every day. Collagen hydrogel was used as a control.

Fourier-transform infrared spectroscopy (FT-IR)

FT-IR spectra of each hydrogel were obtained to determine the retention of HA in the collagen hydrogel. Using an attenuated total reflection infrared spectrometer (ATR-FTIR, Bruker Tensor27) at a range of 4000 to 650 cm^{-1}, spectra were recorded. For comparison, freeze-dried crosslinked HA and collagen hydrogel were also analyzed.

Carbazole assay

To determine the retention of crosslinked HA within the hydrogel, release amount of crosslinked HA was measured by the carbazole assay. Non-crosslinked HA was used as a control. Final concentration of 1 % *w/v* of non-crosslinked or crosslinked HA within collagen hydrogel was incubated in distilled water. Water was collected after 6 days and carbazole assay was performed as described previously using known concentrations of D-glucuronic acid to construct the standard curve [21].

Real-time PCR analysis

Gene expression of type I collagen, type II collagen, and aggrecan were analyzed after 3 weeks of culture within hydrogel constructs (n=3). Total RNA was extracted from each hydrogel with Trizol and reverse transcribed into cDNA using M-MLV cDNA synthesis kit according to the manufacturer's instructions. Using SYBR Green PCR Mastermix and ABI StepOnePlus™ Real time PCR system, cDNA was amplified by rabbit specific primer for type I collagen, type II collagen, and aggrecan. GAPDH was used as a control and gene expression level was calculated as $-2^{\Delta\Delta Ct}$. The rabbit specific primers are listed below in Table 1.

Histological analysis

After 3 weeks of culture of fibrochondrocyte within hydrogels, constructs were fixed in 4 % paraformaldehyde, snap-frozen in OCT embedding media cooled by liquid nitrogen, and cryosectioned into 10-μm-thick sections. Sections were stained with hematoxylin for 3 min followed by Eosin Y staining for 1 min. For Safranin-O staining, sections were stained with 0.1 % Safranin-O solution after hematoxylin staining for 3 min. Sections were also stained with Masson's trichrome for collagen detection.

Statistical analysis

All data are presented as mean±standard deviation (SD). Statistical significance between groups was determined by Student's t test using Microsoft Excel with $*p<0.05$, $**p<0.01$, and $***p<0.005$.

Results

Preparation and characterization of photo-crosslinked collagen hydrogels

Acid dissolved collagen solution can form physical crosslinking upon neutralization and 37 °C incubation. In order to deduce the riboflavin (RF)-induced chemical crosslinking, we have utilized a two-step gelation method [17] (Fig. 1). First, neutralized collagen solution was incubated at 37 °C to form self-assembled triple intrahelical crosslinks [22]. The incubation time was varied from 10 to 20 min for a partial physical crosslinking of collagen to a full physical crosslinking. Physical crosslinking of collagen via neutralization and 37 °C incubation resulted in collagen hydrogel, which retained its fluid-like property. Subsequently, collagen hydrogel was exposed to UV (3.5 mW/cm^2) along with RF for covalent crosslinking between amino acids of collagen fibril. RF-mediated photo-crosslinked collagen hydrogel showed stiffer materials property with defined shape—control compared to the physical-crosslinked collagen hydrogels. In the presence of oxygen and UV light, riboflavin can induce intrahelical crosslinking of amino acids, such as arginine, histidine, and lysine.

We further sought to determine the appropriate RF concentration to fabricate photo-crosslinked collagen hydrogels (COL-RF) with improved mechanical property compared to physically crosslinked collagen hydrogels (COL). Photo-crosslinking of collagen with RF concentration of 0.001, 0.005, 0.01, 0.02, and 0.1 % were examined, and frequency sweep measurements were performed with 3 min UV exposure (Fig. 2). In Fig. 2, the results indicated that photo-crosslinking with RF could significantly increase elastic modulus of collagen. In addition, there was a continuous increase of elastic modulus in the COL with greater dependency on frequency. In contrast, COL-RF exhibited consistent elastic modulus value in a range of frequency 0.1 to 100 Hz demonstrating more elastic behavior than COL. The results also indicate that the optimal RF concentration to increase the modulus of the constructs were 0.01 %, which was 5.5 times stiffer than the COL at frequency of 0.25 rad/s (Supplementary Fig. 1).

We further examined the effect of incubation time prior to UV exposure. Neutralized collagen solutions were incubated in 37 °C for 10 or 20 min prior to UV exposure (1, 3, or 5 min) (Fig. 3a). As incubation time was increased from 10 to 20 min, hydrogel became cloudy, which indicates increased triple helix formation. Duration of UV exposure time did not influence the hydrogel appearance. To determine triple helix formation on the incubation for 10 and 20 min, we carried out circular dichroism (CD) measurements (Fig. 3b). Collagen solution (in acidic condition), COL (physically crosslinked collagen), and COL-RF (riboflavin-induced photo-crosslinked collagen) that were incubated in 37 °C for 10 or 20 min prior to UV exposures were analyzed. For COL-RF, UV exposure time was fixed to 3 min. COL exhibited a negative peak at 190 nm and a positive peak at 230 nm, which is the characteristic of triple helix structure of native collagen [23]. Similarly, CD spectra of COL-RF with 10 or 20 min of incubation showed maximum peak at 230 nm and minimum peak at 190 nm. The

Table 1 Primer list

Gene	Primer 5′–3′
GAPDH	F: TCA CCA TCT TCC AGG AGC GA
	R: CAC AAT GCC GAA GTG GTC GT
Type I collagen	F: CTG ACT GGA AGA GCG GAG AGT AC
	R: CCA TGT CGC AGA AGA CCT TGA
Type II collagen	F: TTC ATG AAG ATG ACC GAC GA
	R: GAC ACG GAG TAG CAC CAT CG
Aggrecan	F: CCT TGG AGG TCG TGG TGA AAG G
	R: AGG TGA ACT TCT CTG GCG ACG T

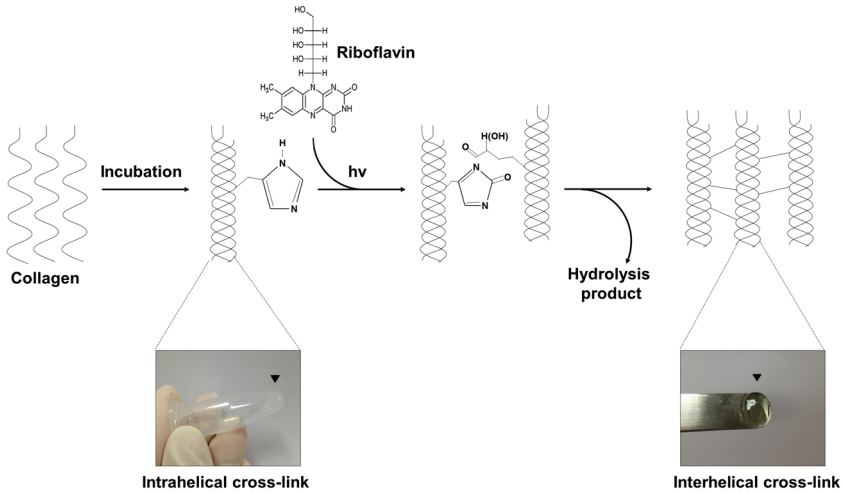

Fig. 1 Schematic representation of photo-crosslinking of collagen with riboflavin. For the first step, collagen precursor solution was incubated to form intrahelical crosslink. Next, samples were UV-treated to form interhelical crosslink between collagen fibril

results demonstrated COL-RF retained a triple helix structure regardless of pre-incubation time.

Hydrogels were further characterized for water retention rate (Fig. 3c). COL had a swelling ratio of 104, which was higher than other COL-RF groups. In addition, pre-incubation duration prior to photo-crosslinking did not alter the swelling ratio. Collagen gels that were treated with RF and UV lights had a significant higher initial viscosity. Furthermore, COL-RF showed a small but significant increase in elastic modulus (Fig. 3d, e). As the incubation and exposure time increased, elastic modulus displayed a tendency to increase. In particular, elastic modulus of constructs was highly increased when incubated for 20 min and UV exposure for 3 and 5 min. For all samples, loss modulus, which signifies viscous dissipation of energy, was nearly an order of magnitude lower than the storage modulus. This result suggests that collagen gels behaved predominantly as solid-like structures.

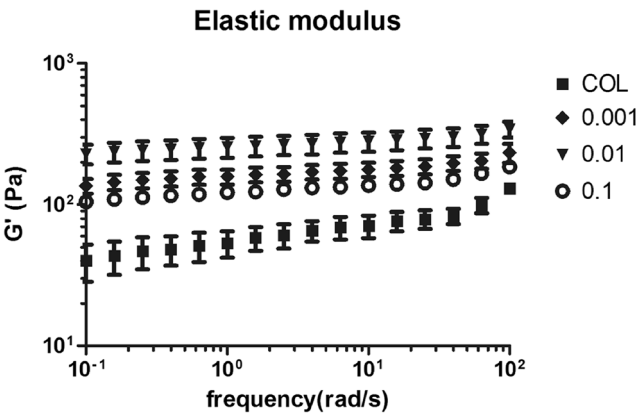

Fig. 2 Mechanical property of riboflavin-induced photo-crosslinking of collagen hydrogels. Elastic modulus analysis of riboflavin-induced photo-crosslinked collagen (COL-RF) vs. collagen (COL). Frequency sweep measurements were performed for hydrogel samples with various amounts of RF. *Error bars* represent the standard deviation from the mean for $n=3$

Next, biocompatibility of the scaffold depending on UV exposure time was examined by encapsulating rabbit fibrochondrocytes within COL-RF (Fig. 3f, g). Free radicals produced during photopolymerization can cause cell death. COL-RF with fibrochondrocytes was exposed with UV for 1, 3, and 5 min, respectively, and viability assay was performed within 24 h. Cell viability was approximately 93–94 % for both 1 and 3 min, and no significant differences were found between two conditions. However, when the cells were exposed to UV for a longer period (5 min), cell viability dramatically decreased to 70 %. Such result indicates that RF affects cell viability when irradiation time exceeds 5 min. Thus, further in vitro studies were performed with 20 min incubation followed by 3 min UV exposure time, which showed improved mechanical properties and higher viability.

Contraction assay and degradation rate analysis

To evaluate cell-mediated hydrogel contractions, 7×10^5 fibrochondrocytes were encapsulated in COL and COL-RF hydrogels (Fig. 4a, b). For COL hydrogel, cell-mediated hydrogel contraction was immediately evident as the diameter of the COL hydrogel resulted in less than 60 % of its original size within 4 h. In contrast, COL-RF hydrogel resisted the fibrochondrocyte-mediated contraction, and the COL-RF hydrogel retained 90 % of its original size even after 66 h (Fig. 4b).

We further explored enzyme-mediated degradation on COL and COL-RF hydrogels (Fig. 4c). COL and COL-RF hydrogels were submerged in 0.1 mg/ml of type I collagenase and incubated at 37 °C. The remaining hydrogel mass were measured at each time point. The weight of the COL hydrogel significantly reduced compared to that of COL-RF hydrogel. Furthermore, COL-RF hydrogels were more resistant and showed increased stability compared to COL in an enzymatically active environment.

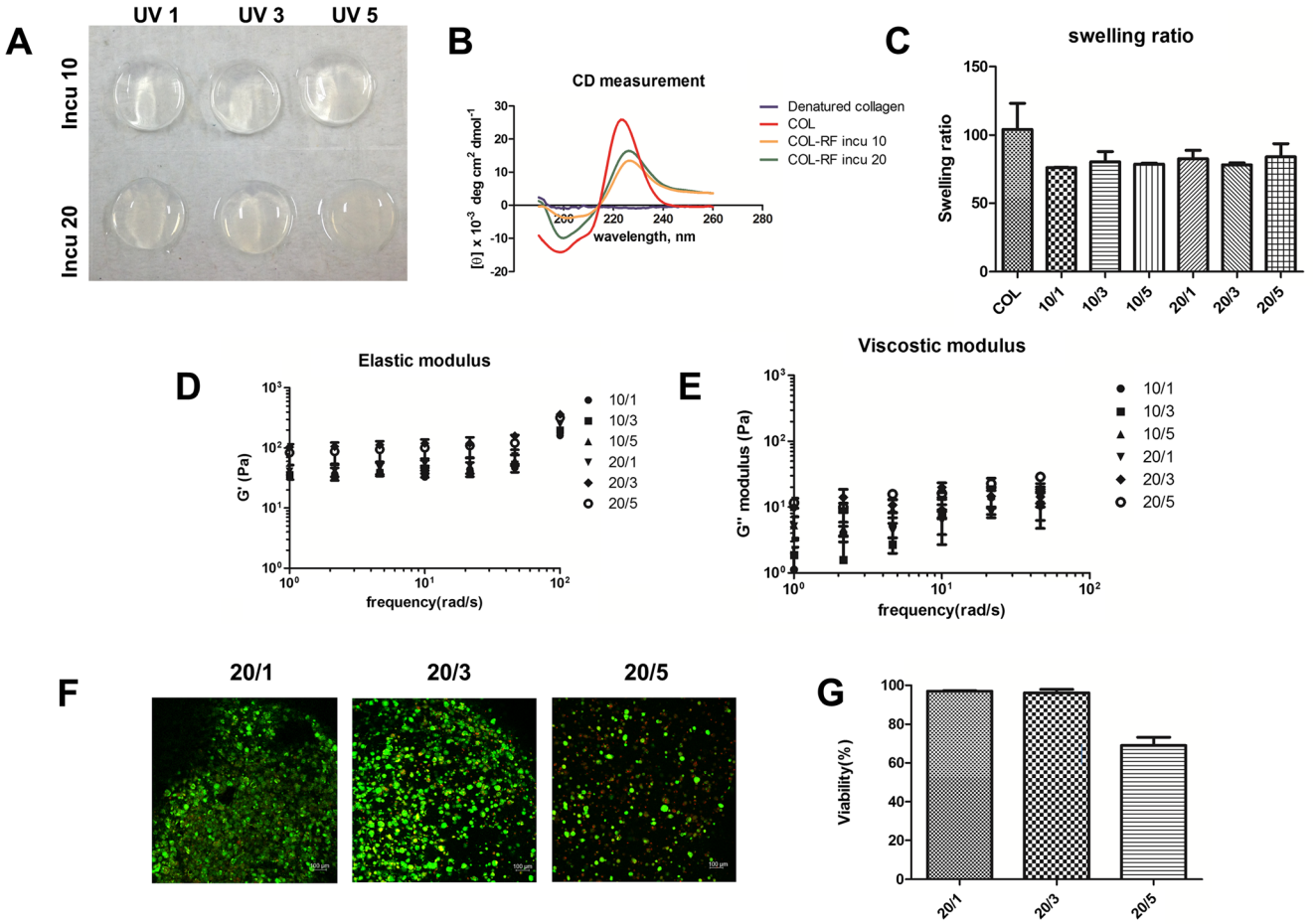

Fig. 3 Incubation and UV exposure time-dependent characterization of photo-crosslinked collagen hydrogel. **a** Gross images of acellular hydrogel. **b** CD measurement of denatured collagen (COL-acetic), collagen hydrogel without riboflavin (COL), and collagen hydrogel with riboflavin (COL-RF) incubated for 10 or 20 min. **c** Swelling ratio of each hydrogel groups and collagen gel without riboflavin was used as a control. *Error bars* represent the standard deviation on the mean for $n=3$. **d** Elastic modulus of the six hydrogel groups with different treatment times. The *left side* of the *slash* means incubation time and the *right side* of the *slash* means UV exposure time. **e** Viscosity modulus of the six hydrogel groups with different treatment times. **f** Influence of UV exposure time on cell viability was assessed through live/dead viability cytotoxicity kit. Live cells were stained green color by Calcein AM and dead cells were stained red color by Ethd-1. *Scale bar*=100 μm. **g** Viability was calculated by the ratio of live cell and total cell number. *Error bars* represent the standard deviation on the mean for $n=3$

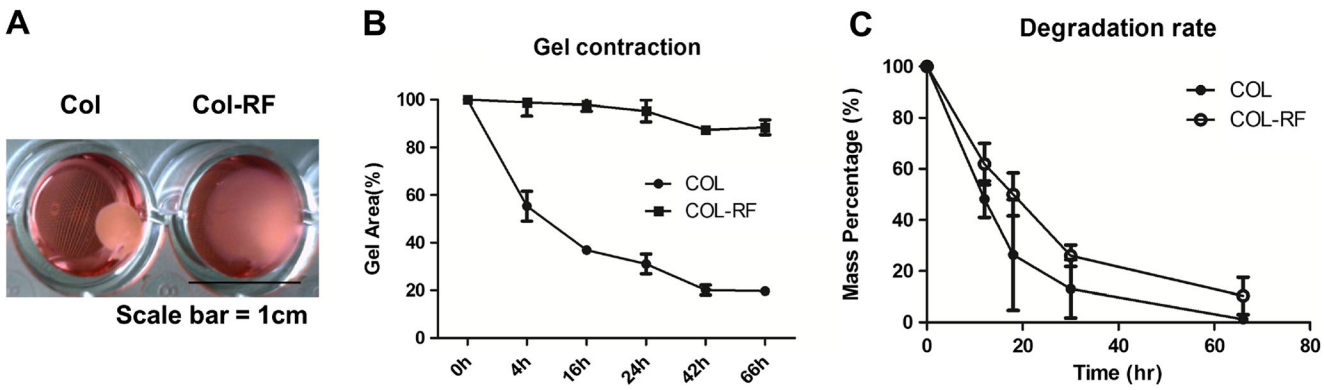

Fig. 4 Cell-mediated collagen hydrogel contraction analysis. **a** Gross appearance of contracted hydrogels containing fibrochondrocyte after 4 h of encapsulation. **b** Comparison of contraction rate between collagen hydrogel (COL) and riboflavin-induced photo-crosslinked hydrogel (COL-RF). The change of gel area was analyzed by measurement of the maximum gel diameter. *Error bars* represent the standard deviation on the mean for $n=3$. **c** Effect of riboflavin-induced photo-crosslinked collagen gel on enzymatic degradation. After treatment with type I collagenase, the mass of remaining construct was measured. *Error bars* represent the standard deviation on the mean for $n=3$

Incorporation of crosslinked HA into COL-RF

HA was introduced to collagen hydrogel to supplement advantageous bioactive factors for meniscus regeneration. Also, in order to continuously retain HA in COL-RF, crosslinked HA was used (Fig. 5a) (Supplementary Fig. 2). With support from EDC and HOBt, HMDA was reacted as a crosslinker between carboxylic acid groups in the HA repeating unit. Moreover, at the end of the reaction, products were dialyzed, freeze-dried, and split into powder form. Powder-formed crosslinked HA was mixed with collagen precursor solution and incubated for 20 min and UV irradiated for 3 min. HA incorporated within COL-RF (COL-RF-HA) was formed in the shape of a small bead that was visible to the naked eye.

To determine HA retention within construct, we conducted carbazole assay and FT-IR. First, carbazole assay was performed to determine the released amount of crosslinked HA (XLHA) from COL-RF (Fig. 5b). Non-crosslinked HA (Non XLHA) incorporated into COL-RF was used as a control. Initial amount of HA was 1.5 mg/construct and each sample was immersed in distilled water for 6 days. After 6 days, distilled water was collected and then the released amount of HA was analyzed by carbazole. As a result, XLHA and non-XLHA exhibited mass percentage of released HA of 4.49 and 31.41 %, respectively.

Furthermore, we performed FT-IR measurements for structural analysis of COL-RF-HA to confirm HA existence within the hydrogel after 7 days (Fig. 6c). XLHA and COL-RF were analyzed for comparison. In the COL-RF-HA spectrum, peaks at 1252 and 1408 cm^{-1} can be attributed to glucuronic acid and symmetric C–O stretching modes of planar carboxyl groups in hyaluronic acid as previously reported [24].

Gene expression analysis and histological staining of fibrochondrocytes in COL and COL-RF

Isolated rabbit fibrochondrocytes (P2) were encapsulated in COL hydrogel, COL-RF hydrogel, and COL-RF-HA hydrogel and cultured for 3 weeks. Real-time PCR was performed for 3-week cultured fibrochondrocytes within three groups of collagen hydrogels: COL, COL-RF, and COL-RF-HA (Fig. 6a). To assess whether fibrochondrocytes in each hydrogel can promote ECM production, expression of type I

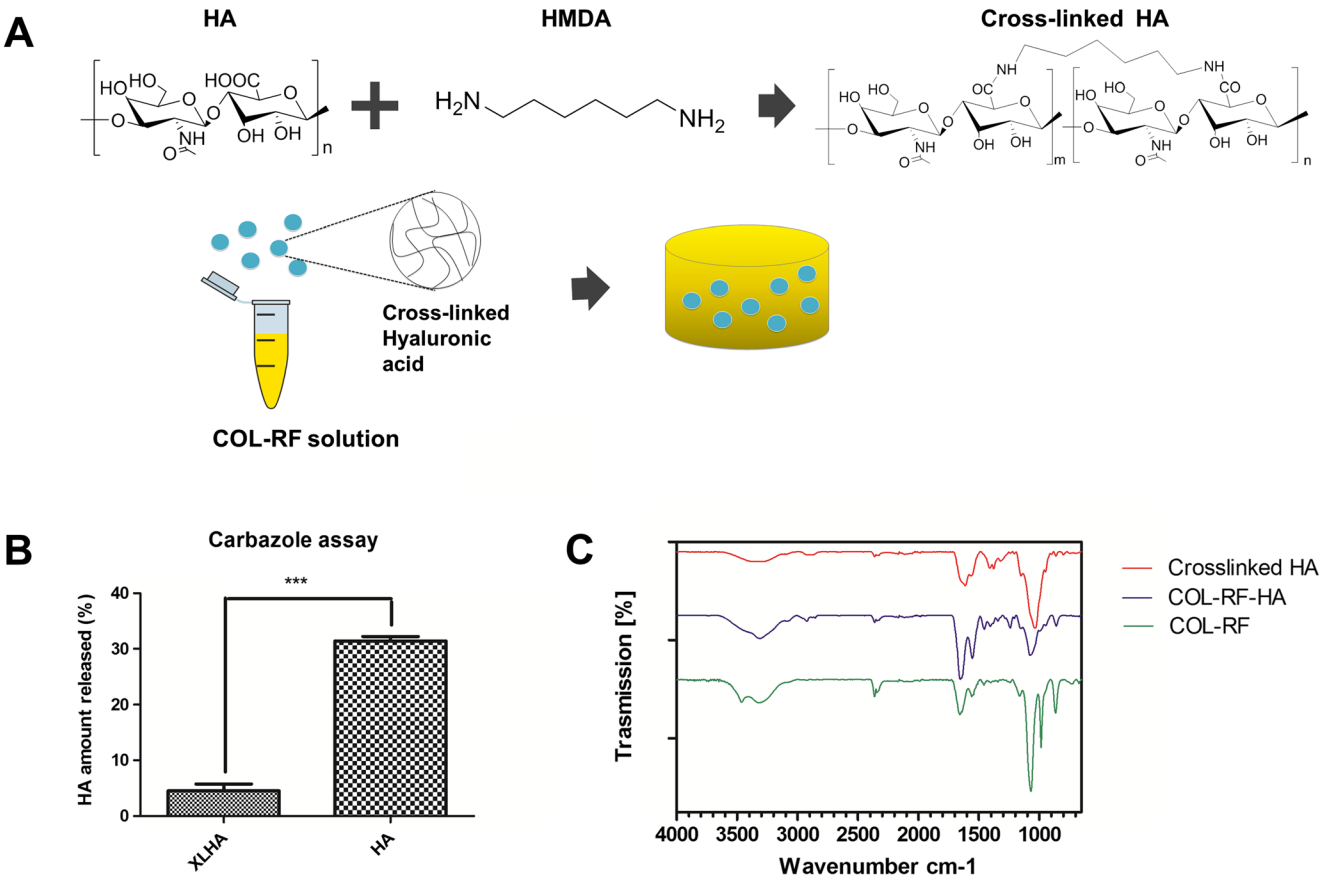

Fig. 5 Synthesis of crosslinked-HA and retention within COL-RF. **a** Schematic representation of the synthesis of crosslinked HA and application in collagen hydrogel. **b** Carbazole assay for confirming the release amount of crosslinked HA from hydrogel. Non-crosslinked HA was used as a control. **c** FT-IR spectra of crosslinked HA, photo-crosslinked collagen hydrogel with crosslinked HA or without HA. ***$p<0.005$

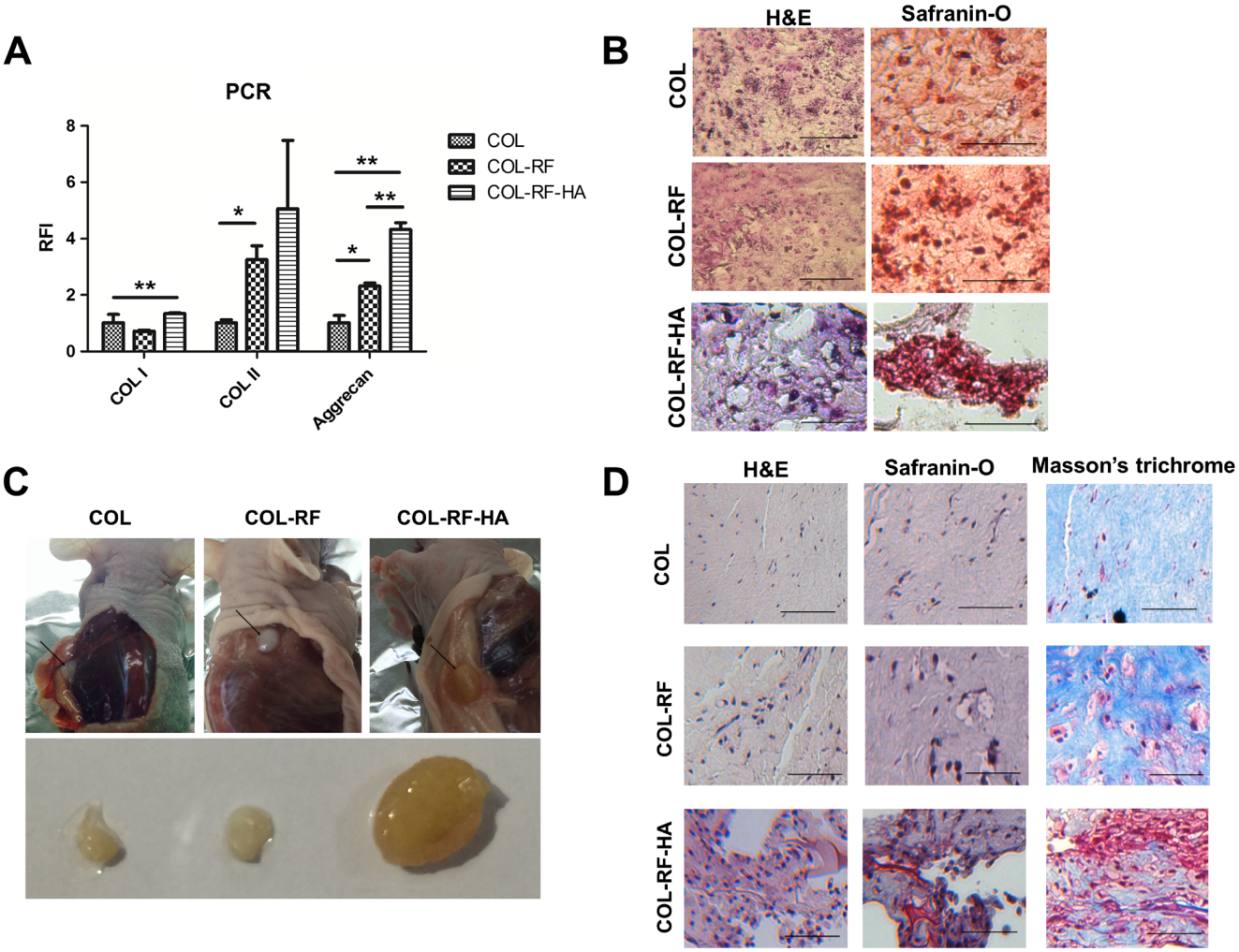

Fig. 6 In vitro and in vivo tissue analysis. **a** Relative gene expression level for meniscus-related factors, collagen I, collagen II, and aggrecan after 3 weeks of rabbit fibrochondrocyte culture within each construct. Gene expression was normalized by collagen hydrogel of day 1 culture. *Error bars* represent the standard deviation on the mean for $n=3$. **b** H&E staining and Safranin-O staining (Saf-O) of rabbit fibrochondrocyte populated hydrogel after 3 weeks' culture. *Scale bar*=100 μm. **c** Gross image of fibrochondrocyte encapsulated COL, COL-RF, and COL-RF-HA constructs after 4 weeks of implantation. **d** H&E staining, Safranin-O (Saf-O) staining, and Masson's trichrome staining analysis of in vivo engineered tissues. *Scale bar*=100 μm. *$p<0.05$, **$p<0.01$

collagen, type II collagen, and aggrecan was analyzed. COL-RF-HA group showed an increase in the gross gene expression level compared to other two groups. Above all, except for type I collagen expression that slightly decreased in COL-RF, there was a significant increase in COL-RF-HA. Also, aggrecan gene expression was significantly elevated in COL-RF-HA compared to COL and COL-RF. For the evaluation of ECM matrix production, histologic sections of each hydrogel populated with 3-week cultured fibrochondrocytes were stained by H&E and Saf-O (Fig. 6b). Larger cellular aggregations were found in COL-RF-HA compared to COL-RF hydrogels. After 3 weeks in culture, sGAG, one of the main cartilaginous ECM components, was expressed more intensely in COL-RF-HA hydrogels compared to in COL-RF and COL, as assessed by Safranin-O staining. These results suggest that HA enhances cartilaginous ECM production in RF-induced photo-crosslinked hydrogel system.

In vivo meniscus regeneration

The feasibility of COL hydrogel, COL-RF hydrogel, and COL-RF-HA hydrogel to support in vivo tissue formation was further investigated. Rabbit fibrochondrocytes were encapsulated in COL, COL-RF, and COL-RF-HA hydrogels, and they were subcutaneously implanted into nude mice for 4 weeks. COL-RF-HA hydrogel retained its original shape over 4 weeks (Fig. 6c). Fibrocartilaginous ECM deposition was evaluated by histological analysis (Fig. 6d). Histological staining revealed a high cell density in the COL-RF-HA hydrogels, while the cellular density remained low in COL and COL-RF. In addition, gross image of host cell infiltration

was observed in the periphery of the COL-RF-HA hydrogels (Supplementary Fig. 3). As observed in vitro, COL-RF-HA showed significantly enhanced cellularity and Safranin-O positive staining compared to other hydrogels, thus confirming HA-induced proteoglycan secretion.

Discussion

This study represents a preliminary step towards the development of a medical technology for use in meniscus repair using photo-oxidation via RF as a photosensitizer. Previously, RF-promoted photo-oxidation has been applied to periodontal wound healing using a dental curing light [25]. Furthermore, RF-based collagen crosslinking is currently being used for cornea tissue and cartilage tissue engineering [26, 27]. Our results support the notion that collagenous biomaterials can be rapidly photo-crosslinked when exposed to UV light in the presence of RF.

Type I collagen is the primary component of the meniscus. The use of collagen as the meniscus scaffold is limited due to rapid degradation, weak mechanical property, and cell-induced collagen hydrogel contraction. To overcome this limitation of collagen hydrogel, we introduced RF-induced photo-crosslinking method on collagen hydrogel. RF serves as a photo-sensitizer inducing production of oxygen radicals that mediate a strong covalent bond between amino acid of collagen fibril [28, 29]. When exposed to light, RF generates reactive oxygen species. Collagen crosslinking via RF and UVA (320–400 nm) is mediated by radical intermediate, such as superoxide, which are formed by triplet state excited RB by absorbed light. The finding of this study has yielded that cell viability was markedly decreased when fibrochondrocytes within COL-RF were exposed to UV over 5 min, probably due to free radicals generated during UV exposure. Considering the viability and elastic modulus, we optimized the RF-induced photo-crosslinked collagen gel for a meniscus scaffold with 0.01 % of RF concentration, 20 min of pre-incubation, and 3 min of UV exposure time.

Spontaneously assembled collagen gel containing cells undergoes rapid contraction by cell–collagen interactions. In that regard, when collagen was used as a tissue engineering scaffold, it could be another limitation along with degradation and weak mechanical property. Ibusuki et al. have shown that the photo-crosslinking can reduce the contraction of COL containing fibroblast or chondrocyte keeping long-term cell viability [30]. Similarly, RF-induced photo-crosslinking of collagen prevented cell-mediated hydrogel contraction. Rheological studies revealed that RF-induced photo-crosslinking increased crosslinking density. The increase of crosslinking density was confirmed by swelling ratio analysis. Furthermore, collagen hydrogel is known to be susceptible to enzymatic degradation. RF-induced photo-crosslinking of collagen resisted collagenase-mediated degradation. A study by R. Zeeman and colleagues has shown that enzymatic degradation can be correlated with interfibrillar and intrafibrillar crosslinks and their density [31]. Thus, the observed result demonstrated that COL-RF has stronger bindings between fibrils than COL. Accordingly, COL-RF is expected to have potential to be used in applications of a meniscus tissue engineering scaffold with well-maintained hydrogel shape and slower degradation rate.

In a load-bearing tissue, such as meniscus, cellular functions are regulated by mechanical signal [32]. Furthermore, meniscus tissue structure is highly organized together with type I collagen, type II collagen, and proteoglycan [33, 34]. Type II collagen network is part of the inner meniscus along with proteoglycan and type I collagen is the main component which accounts for 90 % of collagen in the meniscus [35]. When embedded on collagen hydrogels, meniscus fibrochondrocytes have been shown to increase mRNA transcript levels of fibrochondrogenic markers [36]. In our study, RF-induced photo-crosslinking improved the physical property of collagen gel, which may have modulated the integrin binding and mechanotransduction. Likewise, fibrochondrocytes in COL-RF hydrogels showed increased collagen type II and aggrecan gene expression, although it did not induce type I collagen gene expression.

Efforts to develop active engineered replacements capable of adapting to and integrating with the in vivo environment have gained tremendous interest. HA has been shown to promote healing of meniscus and proliferation [37]. Previous studies on meniscus tissue engineering have shown that HA have potential for stimulating collagen remodeling, healing of the meniscal injury, and producing bizonal tissue similar to meniscus [38–40]. Additionally, Freyman et al. found that the addition of hyaluronic acid induces meniscal matrix formation when cultivated in 3D culture [38]. In the current study, we have incorporated crosslinked HA for increased biological activity. Crosslinked HA is bulky and has little carboxyl group, which is the recognition site of hyaluronidase; crosslinked HA is expected to be more stable than non-crosslinked HA [41, 42] (Supplementary Fig. 2). Through carbazole assay, crosslinked HA retention within COL-RF was confirmed. Our study demonstrated that the fibrochondrocytes encapsulated in COL-RF-HA displayed formation of native meniscus-like tissue. HA-dependent GAG synthesis may have contributed to the increased ECM matrix deposition in COL-RF-HA, while COL-RF showed GAG deposition with surrounding cells that results from less activity on GAG production. However, in vitro histological analysis of COL-RF was different from this result displaying extensive GAG deposition of pericellular region and matrix. The reason for these discrepancies could be the rapid degradation rate in an in vivo environment. Since collagen hydrogel is susceptible to degradation in vivo environment due to the

presence of collagenase, there could be no sufficient time to broaden GAG deposition through the matrix. Based on these findings, we therefore suggest that the addition of COL-RF with crosslinked HA could enhance the fibrochondrocyte function of ECM synthesis. Even though RF-induced photo-crosslinking still provides substantially lower mechanical property than native meniscus tissue, we hypothesize that stress-induced shape deformation of hydrogel would augment its mechanical properties.

Recent scaffold-based therapies are an attractive option to repair damaged meniscus. There is an increasing interest in developing biomaterials systems to recruit cells in the defective area and promote tissue regeneration. RF-induced photo-crosslinked collagen hydrogels may serve as an appropriate delivery modality for living cells due to non-cytotoxicity and short gelation time. Furthermore, incorporation of therapeutic agents, such as HA, to RF-induced photo-crosslinked collagen and efficient delivery to the site of meniscus damage could improve the clinical meniscus repair.

Conclusion

For potential meniscus regeneration, we obtained collagen hydrogel scaffold characterized by delayed degradation, reduced contractility, and improved mechanical property through riboflavin-induced photo-crosslinking. Furthermore, the results of gene expression analysis and histology suggest that fibrochondrocytes may induce the synthesis of GAG after 3 weeks of culture within photo-crosslinked collagen gel. To activate fibrochondrocyte function of meniscal ECM molecule synthesis such as type I collagen, we supplemented crosslinked HA to achieve the desired ECM production. These results indicated that physically improved injectable collagen hydrogel and bioactive HA supplement might be beneficial for scaffold-based meniscus regeneration.

Acknowledgment This research was supported by the Ministry of Health and Welfare of Korea (grant no. HI13C0451020013).

Informed consent All institutional and national guidelines for the care and use of laboratory animals were followed.

References

1. Kawamura S, Lotito K, Rodeo SA. Biomechanics and healing response of the meniscus. Oper Tech Sports Med. 2003;11:68–76.
2. Proctor C, Schmidt M, Whipple R, Kelly M, Mow V. Material properties of the normal medial bovine meniscus. J Orthop Res. 1989;7:771–82.
3. Rath E, Richmond JC. The menisci: basic science and advances in treatment. Br J Sports Med. 2000;34:252–7.
4. Bullough PG, Munuera L, Murphy J, Weinstein AM. The strength of the menisci of the knee as it relates to their fine structure. J Bone Joint Surg Br Vol. 1970;52:564–70.
5. Nakano T, Dodd CM, Scott PG. Glycosaminoglycans and proteoglycans from different zones of the porcine knee meniscus. J Orthop Res. 1997;15:213–20.
6. Arnoczky SP, Warren RF. The microvasculature of the meniscus and its response to injury an experimental study in the dog. Am J Sports Med. 1983;11:131–41.
7. Fayard J-M, Pereira H, Servien E, Lustig S, Neyret P. Meniscectomy: global results—complications. The Meniscus: Springer; 2010. pp. 177–90.
8. Peters G, Wirth CJ. The current state of meniscal allograft transplantation and replacement. Knee. 2003;10:19–31.
9. Burks RT, Metcalf MH, Metcalf RW. Fifteen-year follow-up of arthroscopic partial meniscectomy. Arthroscopy. 1997;13:673–9.
10. Mueller SM, Shortkroff S, Schneider TO, Breinan HA, Yannas IV, Spector M. Meniscus cells seeded in type I and type II collagen–GAG matrices in vitro. Biomaterials. 1999;20:701–9.
11. Gruber HE, Mauerhan D, Chow Y, Ingram JA, Norton HJ, Hanley EN, et al. Three-dimensional culture of human meniscal cells: extracellular matrix and proteoglycan production. BMC Biotechnol. 2008;8:54.
12. Harris Jr ED, Farrell ME. Resistance to collagenase: a characteristic of collagen fibrils cross-linked by formaldehyde. Biochimica et Biophysica Acta (BBA)-Protein Structure. 1972;278:133–41.
13. Van Luyn M, Van Wachem P, Olde Damink L, Dijkstra P, Feijen J, Nieuwenhuis P. Relations between in vitro cytotoxicity and crosslinked dermal sheep collagens. J Biomed Mater Res. 1992;26:1091–110.
14. Hovakimyan M, Guthoff RF, Stachs O. Collagen cross-linking: current status and future directions. J Ophthalmol. 2012;2012,406850.
15. Spörl E, Huhle M, Kasper M, Seiler T. Increased rigidity of the cornea caused by intrastromal cross-linking. Der Ophthalmologe: Zeitschrift der Deutschen Ophthalmologischen Gesellschaft. 1997;94:902–6.
16. Zhang Y, Conrad AH, Conrad GW. Effects of ultraviolet-A and riboflavin on the interaction of collagen and proteoglycans during corneal cross-linking. J Biol Chem. 2011;286:13011–22.
17. Tirella A, Liberto T, Ahluwalia A. Riboflavin and collagen: new crosslinking methods to tailor the stiffness of hydrogels. Mater Lett. 2012;74:58–61.
18. Choi B, Kim S, Lin B, Li K, Bezouglaia O, Kim J, et al. Visible-light-initiated hydrogels preserving cartilage extracellular signaling for inducing chondrogenesis of mesenchymal stem cells. Acta Biomater. 2015;12:30–41.
19. Sonoda M, Harwood FL, Amiel ME, Moriya H, Temple M, Chang DG, et al. The effects of hyaluronan on tissue healing after meniscus injury and repair in a rabbit model. Am J Sports Med. 2000;28:90–7.
20. Yeom J, Bhang SH, Kim B-S, Seo MS, Hwang EJ, Cho IH, et al. Effect of cross-linking reagents for hyaluronic acid hydrogel dermal fillers on tissue augmentation and regeneration. Bioconjug Chem. 2010;21:240–7.
21. Bitter T, Muir HM. A modified uronic acid carbazole reaction. Anal Biochem. 1962;4:330–4.
22. Lee JM, Pereira CA, Kan LW. Effect of molecular structure of poly (glycidyl ether) reagents on crosslinking and mechanical properties of bovine pericardial xenograft materials. J Biomed Mater Res. 1994;28:981–92.
23. Cooper NR. The classical complement pathway: activation and regulation of the first complement component. Adv Immunol. 1985;37:151–216.

24. Wu Y. Preparation of low-molecular-weight hyaluronic acid by ozone treatment. Carbohydr Polym. 2012;89:709–12.
25. Brennan-Pierce EP, MacAskill I, Price RB, Lee JM. Riboflavin-sensitized photo-crosslinking of collagen using a dental curing light. Bio-Med Mater Eng. 2014;24:1659–71.
26. Choi B, Kim S, Lin B, Li K, Bezouglaia O, Kim J, et al. Visible-light-initiated hydrogels preserving cartilage extracellular signaling for inducing chondrogenesis of mesenchymal stem cells. Acta Biomater. 2015;12C:30–41.
27. Konstantopoulos A, Mehta JS. Conventional versus accelerated collagen cross-linking for keratoconus. Eye Contact Lens. 2015;41:65–71.
28. Voicescu M, Ionita G, Constantinescu T, Vasilescu M. The oxidative activity of riboflavin studied by luminescence methods: the effect of cysteine, arginine, lysine and histidine amino acids. Rev Roum Chim. 2006;51:683–90.
29. Raiskup F, Spoerl E. Corneal crosslinking with riboflavin and ultraviolet A. I. Principles. Ocul Surf. 2013;11:65–74.
30. Ibusuki S, Halbesma GJ, Randolph MA, Redmond RW, Kochevar IE, Gill TJ. Photochemically cross-linked collagen gels as three-dimensional scaffolds for tissue engineering. Tissue Eng. 2007;13:1995–2001.
31. Zeeman R, Dijkstra PJ, van Wachem PB, van Luyn MJ, Hendriks M, Cahalan PT, et al. Successive epoxy and carbodiimide cross-linking of dermal sheep collagen. Biomaterials. 1999;20:921–31.
32. Han W, Heo S, Driscoll T, Boggs M, Duncan R, Mauck R, et al. Impact of cellular microenvironment and mechanical perturbation on calcium signalling in meniscus fibrochondrocytes. Eur Cells Mater. 2014;27:321–31.
33. Chevrier A, Nelea M, Hurtig MB, Hoemann CD, Buschmann MD. Meniscus structure in human, sheep, and rabbit for animal models of meniscus repair. J Orthop Res. 2009;27:1197–203.
34. Hasan J, Fisher J, Ingham E. Current strategies in meniscal regeneration. J Biomed Mater Res B Appl Biomater. 2014;102:619–34.
35. Eyre D, Koob T, Chun L. Biochemistry of the meniscus: unique profile of collagen types and site-dependent variations in composition. Orthop Trans. 1983;8:56.
36. Croutze R, Jomha N, Uludag H, Adesida A. Matrix forming characteristics of inner and outer human meniscus cells on 3D collagen scaffolds under normal and low oxygen tensions. BMC Musculoskelet Disord. 2013;14:353.
37. Ishima M, Wada Y, Sonoda M, Harada Y, Katsumi A, Moriya H. Effects of hyaluronan on the healing of rabbit meniscus injured in the peripheral region. J Orthop Sci. 2000;5:579–84.
38. Freymann U, Endres M, Goldmann U, Sittinger M, Kaps C. Toward scaffold-based meniscus repair: effect of human serum, hyaluronic acid and TGF-β3 on cell recruitment and re-differentiation. Osteoarthr Cartil. 2013;21:773–81.
39. Tan G-K, Dinnes DL, Butler LN, Cooper-White JJ. Interactions between meniscal cells and a self assembled biomimetic surface composed of hyaluronic acid, chitosan and meniscal extracellular matrix molecules. Biomaterials. 2010;31:6104–18.
40. Marsano A, Vunjak-Novakovic G, Martin I. Towards tissue engineering of meniscus substitutes: selection of cell source and culture environment. Conf Proc IEEE Eng Med Biol Soc. 2006;1:3656–8.
41. Chao KL, Muthukumar L, Herzberg O. Structure of human hyaluronidase-1, a hyaluronan hydrolyzing enzyme involved in tumor growth and angiogenesis. Biochemistry. 2007;46:6911–20.
42. Yan XM, Seo MS, Hwang EJ, Cho IH, Hahn SK, Sohn UD. Improved synthesis of hyaluronic acid hydrogel and its effect on tissue augmentation. J Biomater Appl. 2011;27:179–86.